

# Iron phthalocyanine nanorods for ethanol sensing

Xiuhua Wang<sup>1,2</sup>, Xiuqin Wang<sup>3</sup>, Jie Gao<sup>1</sup>, Bingang Xu<sup>2</sup> ✉

<sup>1</sup>The Key Laboratory of Functional Molecular Solids, Ministry of Education, College of Chemistry and Materials Science, Anhui Normal University, Wuhu 241000, People's Republic of China

<sup>2</sup>Nanotechnology Center, Institute of Textiles and Clothing, The Hong Kong Polytechnic University, Hung Hom, Kowloon, Hong Kong

<sup>3</sup>Department of Anesthesiology, Shandong Cancer Hospital affiliated to Shandong University, Shandong Academy of Medical Science, Jinan 250117, People's Republic of China

✉ E-mail: txsubg@polyu.edu.hk

Published in Micro & Nano Letters; Received on 13th March 2016; Revised on 11th April 2016; Accepted on 12th April 2016

Iron phthalocyanine (FePc) nanorods were synthesised by a solvothermal method without any surfactant. The as-synthesised materials were monoclinic FePc phase according to X-ray diffraction. The FePc nanorods were applied as gas sensor to detect the ethanol with good sensitivity and selectivity. The results demonstrated that FePc nanorods were excellent candidates for gas sensor to ethanol.

**1. Introduction:** As organometallic compounds semiconductors, metal phthalocyanine (MPc) has attracted much interest because of their unique optical and electronic properties, which are fundamentally different from those of inorganic ones [1–4]. MPc has two strong absorption peaks, one of which is observed at ca. 300–500 nm and the other in about 600–750 nm. MPcs are highly thermal and chemical stable molecules, resistant to oxidation, which are mainly used as photovoltaic cell elements, solid-state sensors and electrochromic devices [5–8]. As an important p-type semiconductor, MPc has been largely investigated in the gas-sensors application owing to the conductivity varying substantially with the concentration of reducing or oxidising gases [9]. Many research of MPc-based gas sensors focused on the solid thin films synthesised by various methods such as thermal evaporation [10], Langmuir–Blodgett (LB) method [11], molecular beam deposition [12], electrochemical deposition and solvothermal method [13].

MPc nanomaterials were found to have outstanding redox and electronic properties that were interesting in gas-sensors applications, active material for molecular electronic devices, photodetectors and photocatalytic catalyst [14–18]. It is found that the gas-sensor performance of MPc strongly depends on its microstructure [19–21]. For example, copper (Cu) Pc nanoribbons based gas sensor showed high reversibility and response to tetrahydrofuran atmosphere [22]. Poly-Cu tetraaminoPc nanotubes as the sensor exhibited fast sensitivities and enhanced linear ranges [23]. CuPc nanostructures were investigated on various technologically important substrates and exhibited selectivity and sensitivity to NO<sub>x</sub> gas as gas-sensing devices [24]. However, iron Pc (FePc) nanorods with sensitivity and selectivity toward ethanol have rarely been reported.

In our Letter, we prepared FePc nanorods via a facile solvothermal method without any surfactant. The as-obtained FePc nanorods exhibited high selectivity and sensitivity to ethanol as gas sensors.

## 2. Experimental section

**2.1. Reagents:** Phthalonitrile (C<sub>8</sub>H<sub>4</sub>N<sub>2</sub>), ferrous chloride (FeCl<sub>2</sub>·6H<sub>2</sub>O), ammonium heptamolybdate [(NH<sub>4</sub>)<sub>6</sub>Mo<sub>7</sub>O<sub>24</sub>·4H<sub>2</sub>O], ethanol and ethylene glycol were in analytical grade and were used directly, commercially available in the Sinopharm Chemical Reagent Co.

**2.2. Preparation of FePc:** Under the magnetic stirring, 0.115 g C<sub>8</sub>H<sub>4</sub>N<sub>2</sub> was dissolved in the 30 ml ethylene glycol mixed

solution, and then 0.054 g FeCl<sub>2</sub>·6H<sub>2</sub>O and 0.001 g (NH<sub>4</sub>)<sub>6</sub>Mo<sub>7</sub>O<sub>24</sub>·4H<sub>2</sub>O were added into the above solution. The mixture was transferred to a 50 ml teflon-lined stainless steel autoclave after stirred uniformly. The sealed autoclave was heated at 180°C for 20 h. Finally, the as-prepared sample was washed by deionised water and absolute ethanol until the filtrate was clear. The product was vacuum dried at 60°C for 24 h.

**2.3. Characterisation of material:** A Philips X'pert PRO MPD diffractometer X-ray diffraction (XRD) equipped with Cu K $\alpha$  radiation was used to investigate the crystal structure and phase of the as-synthesised samples. A Hitachi S-4800 field emission scanning electron microscopy (FESEM) was used to investigate the morphologies of the samples. Transmission electron microscope (TEM) was recorded using a Tecnai G2 F20 high-resolution TEM analyser. Differential thermal gravity (DTG) and thermogravimetric analysis (TGA) were taken with a SETARAM-TG92 thermal gravimetric (TG) analyser under nitrogen flow.

**2.4. Fabrication and measurement of gas sensors:** The layouts of the sensor are the same to our previous report [25]. The slurry was formed by the mixture of the FePc nanorods and ethanol. The gas sensor was prepared by coating the slurry onto a ceramic tube with four platinum wires and a pair of golden electrodes, and then dried in air. The Cr–Ni alloy filaments were plugged into the tube employed as a heating appliance that afforded the working temperature of the gas sensor. FePc nanorods (5.0 mg) were directly coated on the outer surface of the ceramic tube and connected the two Au electrodes, then dried in air. Detecting gases were injected into a shielded chamber. The responses property of the gas sensor was investigated using a WS-30A test gas-sensing system at relative humidity of 40–60%. The sensor sensitivity is defined as  $S = R_g/R_a$ , where  $R_g$  is the electrical resistance in test gas and  $R_a$  is the resistance in air.

## 3. Results and discussion

**3.1. Characterisation of material:** Fig. 1a displays the XRD peaks of the samples. The diffraction peaks located at  $2\theta = 6.9^\circ, 11.1^\circ, 12.0^\circ, 13.0^\circ, 15.6^\circ, 17.9^\circ, 24.1^\circ, 25.9^\circ$  and  $28.8^\circ$  can be all perfectly indexed as monoclinic FePc (JCPDS Card No 14-0926). The FESEM image displays the morphology of the product. Fig. 1b shows the representative high-magnification SEM morphology of the rod-like FePc with lengths up to 100  $\mu\text{m}$ . A close SEM

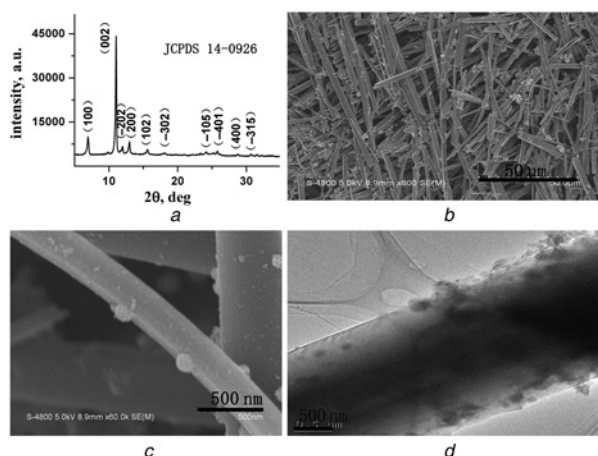


**Fig. 1** Characterisation of material  
*a* XRD peak of the FePc nanorods  
*b* and *c* Low- and high-magnification SEM image of the FePc nanorods  
*d* Photograph of TEM image of the FePc nanorods

examination demonstrates that the diameters of FePc rods are average 700 nm (Fig. 1c). The TEM image further reveals the rod-like nature of the FePc nanorods, as shown in Fig. 1d.

TGA and DTG behaviours of the FePc nanorods were recorded with TG analysis. Fig. 2 displays thermo-decomposition behaviours of the FePc nanorods. On the TGA curve, the first weight loss of 1.5% between 50 and 100°C (endothermic DTG peak at 66°C), attributed to the sublimation of water weakly adsorbed on the surface of the FePc rods. An apparent decomposition step can be clearly observed from the TGA curve. The second weight loss of 45.2% between 233 and 400°C indicates the decomposing of FePc. The DTG graph further displays that the FePc nanorods decomposing temperature is between 310 and 410°C.

**3.2. Gas-sensing measurements:** As we know, the sensitivity of the gas sensor is greatly influenced by the working temperature and the working temperature is an important factor. To obtain the appropriate working temperature, the response of the FePc nanorods sensor to 100 ppm to ethanol vapour in air was measured as a function of working temperature, as shown in Fig. 3. It is clear that the sensitivity of the gas sensor varies with working temperature. The sensitivity first increases with temperature, up to 300°C, and then gradually decreases. The maximum gas-sensor sensitivity of FePc nanorods is found 9.05 at 300°C in our experimental range. So, the appropriate working temperature of 300°C was chosen for examining the gas-sensing characteristics of the as-obtained FePc nanorods.

Fig. 4 shows the response of FePc nanorods based gas-sensor exposure to various amounts of ethanol at the appropriate working temperature of 300°C. The as-obtained FePc nanorods have a

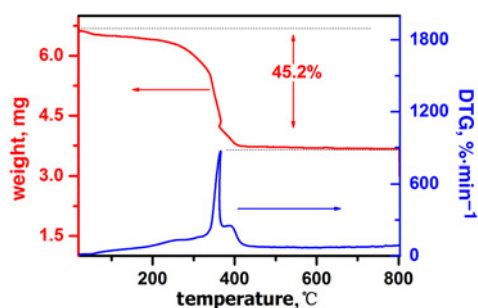


**Fig. 2** DTG and TGA DTG curves of FePc nanorods at a heating rate of temperature of 10°C under nitrogen flow

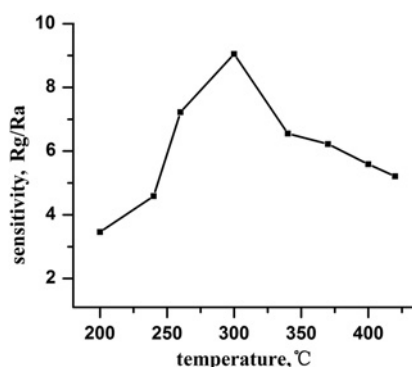


**Fig. 3** Sensitivities of the FePc nanorods gas sensor to 100 ppm ethanol at various operating temperatures

good response to ethanol. As can be observed, the sensitivity increases when the test gas ethanol is added. At a low concentration of 10 ppm ethanol, the relative sensitivity is about 4.3. The starting minimum concentration is 10 ppm, which is down the permissible exposure limits (200 ppm) set of a breath analyser [26]. With increasing the ethanol vapour concentration from 10 to 80 ppm, the responses of the sensor increase rapidly. However, the response increases slowly with increasing the concentrations of ethanol above 80 ppm, which indicates that the response of the FePc nanorods sensor attained a relative saturation value.

As p-type semiconductor, the resistance of the gas sensor in a reducing gas (such as ethanol) is greater than the resistance in the air. When the FePc nanorods sensor is exposed to the air, O<sub>2</sub> adsorbed on the surface of the FePc nanorods capture the electrons from the FePc nanorods, resulting in the production of O<sup>2-</sup> and O<sup>-</sup>. Meanwhile, the hole accumulation layer is formed on the surface of the FePc nanorods. When the sensor touches with ethanol, ethanol molecules react with O<sup>2-</sup> and O<sup>-</sup> and release electrons back to the FePc nanorods. The releasing electrons react with the holes, decreasing the thickness of the hole accumulation layer, thus increasing the resistance of the sensor.

The selectivity of the gas sensor is also very key for the application of the gas sensing. Therefore, the gas selectivity property of FePc nanorods sensor was assessed. Various gases with the same concentration, e.g. ammonia, benzene, acetone, methylbenzene, formaldehyde, isopropanol and ethanol were selected to investigate gas selectivity property of FePc nanorods sensor at the appropriate working temperature of 300°C, as shown in Fig. 5. The FePc nanorods gas sensor presents higher response to ethanol than other gases that indicates that the gas sensor displays fine selectivity to ethanol. Compared with the previous Letter, the sensitivity of FePc nanorods gas sensor to ethanol was higher. We believe that the high sensing behaviour attributed to the remarkable one-dimensional structure of

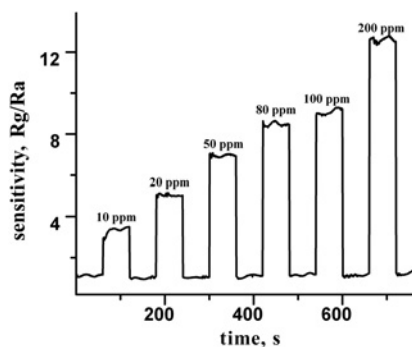


**Fig. 4** Sensitivities of the FePc nanorods gas sensor to different ethanol concentration at the appropriate working temperature of 300°C

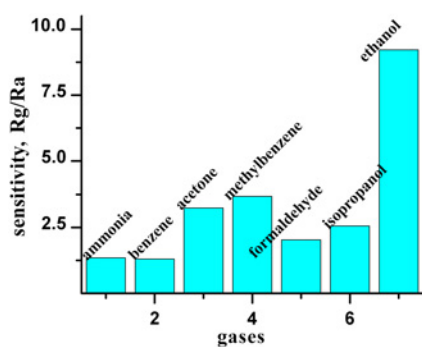


**Fig. 5** Sensitivities of FePc nanorods gas sensor to various gases with a concentration of 100 ppm at 300°C

FePc nanorods, which is favourable for the mass transportation and diffusion in the gas-sensing materials [27].

**4. Conclusion:** The FePc nanorods were synthesised successfully by a facile solvothermal technique without any surfactant. FePc nanorods gas sensor exhibited good response to ethanol with high sensitivity and selectivity due to the 1D morphology. All the data show that the FePc nanorods are suitable for gas sensor to ethanol. The easy synthesis of FePc nanorods, good sensitivity and selectivity of the fabricated sensor are expected to have potential applications of these devices in practical applications.

**5. Acknowledgment:** This work has been supported by the Natural Science Foundation of China (grant no. 21301007).

## 6 References

- [1] Saini R., Mahajan A., Bedi R.K., *ET AL.*: 'Room temperature ppb level Cl-2 detection and sensing mechanism of highly selective and sensitive phthalocyanine nanowires', *Sens. Actuators B, Chem.*, 2014, **203**, pp. 17–24
- [2] Liang X., Chen Z., Wu H., *ET AL.*: 'Enhanced NH<sub>3</sub>-sensing behavior of 2,9,16,23-tetrakis (2,2,3,3-tetrafluoropropoxy) metal(II) phthalocyanine/multi-walled carbon nanotube hybrids: an investigation of the effects of central metals', *Carbon*, 2014, **80**, pp. 268–278
- [3] Fernandez-Sanchez J.F., Fernandez I., Steiger R., *ET AL.*: 'Second-generation nanostructured metal oxide matrices to increase the thermal stability of CO and NO<sub>2</sub> sensing layers based on iron (II) phthalocyanine', *Adv. Funct. Mater.*, 2007, **17**, (7), pp. 1188–1198
- [4] Apetrei C., Medina-Plaza C., Antonio de Saja J., *ET AL.*: 'Electrochemical characterization of dilithium phthalocyanine carbonaceous electrodes', *J. Porphyrins Phthalocyanines*, 2013, **17**, (6–7), pp. 522–528
- [5] Uslan C., Oppelt K.T., Reith L.M., *ET AL.*: 'Characterization of a non-aggregating silicon (IV) phthalocyanine in aqueous solution: toward red-light-driven photocatalysis based on earth-abundant materials', *Chem. Commun.*, 2013, **49**, (73), pp. 8108–8110
- [6] Wang R.-M., Wang H., Wang Y., *ET AL.*: 'Preparation and photocatalytic activity of chitosan-supported cobalt phthalocyanine membrane', *Color Technol.*, 2014, **130**, (1), pp. 32–36
- [7] Li D., Ge S., Huang J., *ET AL.*: 'Photocatalytic chromogenic identification of chlorophenol pollutants by manganese phthalocyanine under sunlight irradiation', *Separation Purification Technol.*, 2014, **125**, pp. 216–222
- [8] Golmojeh H., Zanjanchi M.A., Arvand M.: 'BiVO<sub>4</sub>-silica composites containing cobalt phthalocyanine groups: synthesis, characterization and application in photodegradation of 2,4,6-trichlorophenol', *Photochem. Photobiol.*, 2013, **89**, (5), pp. 1029–1037
- [9] Medina-Plaza C., Revilla G., Munoz R., *ET AL.*: 'Electronic tongue formed by sensors and biosensors containing phthalocyanines as electron mediators. Application to the analysis of red grapes', *J. Porphyrins Phthalocyanines*, 2014, **18**, (1–2), pp. 76–86
- [10] Padma N., Joshi A., Singh A., *ET AL.*: 'NO<sub>2</sub> sensors with room temperature operation and long term stability using copper phthalocyanine thin films', *Sens. Actuators B, Chem.*, 2009, **143**, (1), pp. 246–252
- [11] Capan I., Ilhan B.: 'Gas sensing properties of mixed stearic acid/phthalocyanine LB thin films investigated using QCM and SPR', *J. Optoelectron. Adv. Mater.*, 2015, **17**, (3–4), pp. 456–461
- [12] Siviero F., Coppede N., Pallaoro A., *ET AL.*: 'Hybrid n-TiO<sub>2</sub>-CuPc gas sensors sensitive to reducing species, synthesized by cluster and supersonic beam deposition', *Sens. Actuators B, Chem.*, 2007, **126**, (1), pp. 214–220
- [13] Patois T., Sanchez J.-B., Berger F., *ET AL.*: 'Elaboration of ammonia gas sensors based on electrodeposited polypyrrole-cobalt phthalocyanine hybrid films', *Talanta*, 2013, **117**, pp. 45–54
- [14] Fan J., Zhao Z., Zhu L., *ET AL.*: 'Preparation and photoreduction CO<sub>2</sub> activity of phthalocyanine modified titania catalysts', *Asian J. Chem.*, 2014, **26**, (3), pp. 667–671
- [15] Wu Y., Zhang X., Pan H., *ET AL.*: 'Large-area aligned growth of single-crystalline organic nanowire arrays for high-performance photodetectors', *Nanotechnology*, 2013, **24**, (35)
- [16] Park J.H., Royer J.E., Chagarov E., *ET AL.*: 'Atomic imaging of the irreversible sensing mechanism of NO<sub>2</sub> adsorption on copper phthalocyanine', *J. Am. Chem. Soc.*, 2013, **135**, (39), pp. 14600–14609
- [17] Gao J., Huang G., Du X.: 'Synthesis and self-assemble nanofibers of tetra phenoxy substituted nickel phthalocyanine', *Asian J. Chem.*, 2014, **26**, (6), pp. 1711–1713
- [18] Zhong X., Liu L., Wang X., *ET AL.*: 'A radar-like iron based nanohybrid as an efficient and stable electrocatalyst for oxygen reduction', *J. Mater. Chem. A*, 2014, **2**, (19), pp. 6703–6707
- [19] Saini R., Mahajan A., Bedi R.K., *ET AL.*: 'Phthalocyanine based nanowires and nanoflowers as highly sensitive room temperature Cl-2 sensors', *RSC Adv.*, 2014, **4**, (31), pp. 15945–15951
- [20] Brunet J., Pauly A., Dubois M., *ET AL.*: 'Improved selectivity towards NO<sub>2</sub> of phthalocyanine-based chemosensors by means of original indigo/nanocarbons hybrid material', *Talanta*, 2014, **127**, pp. 100–107
- [21] Luz Rodriguez-Mendez M., Antonio de Saja J.: 'Nanostructured thin films based on phthalocyanines: electrochromic displays and sensors', *J. Porphyrins Phthalocyanines*, 2009, **13**, (4–5), pp. 606–615
- [22] Zhang Y., Hu W.: 'Field-effect transistor chemical sensors of single nanoribbon of copper phthalocyanine', *Sci. China B, Chem.*, 2009, **52**, (6), pp. 751–754
- [23] Gu F., Xu G.Q., Ang S.G.: 'Studies on CuTAPc-nanotube-modified electrodes as chemical sensors for NO', *Nanotechnology*, 2009, **20**, (30)
- [24] Strelcov E., Kolmakov A.: 'Copper phthalocyanine quasi-1D nanostructures: growth morphologies and gas sensing properties', *J. Nanosci. Nanotechnol.*, 2008, **8**, (1), pp. 212–221
- [25] Wang X., Yao S., Wu X., *ET AL.*: 'High gas-sensor and supercapacitor performance of porous Co<sub>3</sub>O<sub>4</sub> ultrathin nanosheets', *RSC Adv.*, 2015, **5**, (23), pp. 17938–17944
- [26] Wen Z., Zhu L., Mei W., *ET AL.*: 'A facile fluorine-mediated hydrothermal route to controlled synthesis of rhombus-shaped Co<sub>3</sub>O<sub>4</sub> nanorod arrays and their application in gas sensing', *J. Mater. Chem. A*, 2013, **1**, (25), pp. 7511–7518
- [27] Huo L.H., Li X.L., Li W., *ET AL.*: 'Gas sensitivity of composite Langmuir-Blodgett films of Fe<sub>2</sub>O<sub>3</sub> nanoparticle-copper phthalocyanine', *Sens. Actuators B, Chem.*, 2000, **71**, (1–2), pp. 77–81